



Development of HEK-293 Cell Lines Constitutively Expressing Flaviviral Antigens for Use in Diagnostics

Jordan A. Powers,^a Benjamin Skinner,^a Brent S. Davis,^a Brad J. Biggerstaff,^a Lucy Robb,^a Elizabeth Gordon,^{a*} William M. de Souza,^b Marcilio Jorge Fumagalli,^c  Amanda E. Calvert,^a Gwong-Jen Chang^a

^aU.S. Centers for Disease Control and Prevention, Fort Collins, Colorado, USA

^bWorld Reference Center for Emerging Viruses and Arboviruses and Department of Microbiology and Immunology, University of Texas Medical Branch, Galveston, Texas, USA

^cCentro de Pesquisa em Virologia, Faculdade de Medicina de Ribeirão Preto, Ribeirão Preto, Brazil

ABSTRACT Flaviviruses are important human pathogens worldwide. Diagnostic testing for these viruses is difficult because many of the pathogens require specialized biocontainment. To address this issue, we generated 39 virus-like particle (VLP)- and nonstructural protein 1 (NS1)-secreting stable cell lines in HEK-293 cells of 13 different flaviviruses, including dengue, yellow fever, Japanese encephalitis, West Nile, St. Louis encephalitis, Zika, Rocio, Ilheus, Usutu, and Powassan viruses. Antigen secretion was stable for at least 10 cell passages, as measured by enzyme-linked immunosorbent assays and immunofluorescence assays. Thirty-five cell lines (90%) had stable antigen expression over 10 passages, with three of these cell lines (7%) increasing in antigen expression and one cell line (3%) decreasing in antigen expression. Antigen secretion in the HEK-293 cell lines was higher than in previously developed COS-1 cell line counterparts. These antigens can replace current antigens derived from live or inactivated virus for safer use in diagnostic testing.

IMPORTANCE Serological diagnostic testing for flaviviral infections is hindered by the need for specialized biocontainment for preparation of reagents and assay implementation. The use of previously developed COS-1 cell lines secreting noninfectious recombinant viral antigen is limited due to diminished antigen secretion over time. Here, we describe the generation of 39 flaviviral virus-like particle (VLP)- and nonstructural protein 1 (NS1)-secreting stable cell lines in HEK-293 cells representing 13 medically important flaviviruses. Antigen production was more stable and statistically higher in these newly developed cell lines than in their COS-1 cell line counterparts. The use of these cell lines for production of flaviviral antigens will expand serological diagnostic testing of flaviviruses worldwide.

KEYWORDS arbovirus, diagnostics, flavivirus, recombinant protein production

Arthropod-borne viruses (arboviruses) in the family *Flaviviridae* cause major public health concerns worldwide, especially as human migration and suitable mosquito habitat evolve as a result of climate change (1). Global incidences of dengue virus (DENV) infections continue to increase with an estimated 390 million infections every year (2), and approximately 53% of the world's population live in areas where DENV transmission may occur (3). Yellow fever virus (YFV) and Japanese encephalitis virus (JEV) demonstrate the difficulties in controlling epizootic diseases despite having effective human vaccines against them, with recurrent outbreaks of yellow fever in sub-Saharan Africa and South America and 68,000 cases of Japanese encephalitis in Asia per year (4, 5). Transmission of West Nile virus (WNV) in Europe was unusually high in 2018 and coincided with circulation of Usutu virus (USUV) (6), a closely related flavivirus. While discovery of other emerging flaviviruses, such as Rocio virus (ROCV) (7), Ilheus virus (ILHV) (8), and Powassan

Editor Manjula Kalia, Regional Centre for Biotechnology

This is a work of the U.S. Government and is not subject to copyright protection in the United States. Foreign copyrights may apply.

Address correspondence to Amanda E. Calvert, zp20@cdc.gov, or Gwong-Jen Chang, gwongjen@gmail.com.

*Present address: Elizabeth Gordon, Colorado State University, Fort Collins, Colorado, USA.

The authors declare a conflict of interest. CDC has filed a patent application describing these cell lines. Davis B.S. and Chang G.J. Stable human cell lines expressing flavivirus virus-like particles and uses thereof, 20 May 2020. US provisional patent application 63/021,852.

[This article was published on 9 May 2022 with a byline that lacked William M. de Souza and Marcilio Jorge Fumagalli. The byline was updated and minor text changes were made in the current version, posted on 6 June 2022.]

Received 17 February 2022

Accepted 13 April 2022

Published 9 May 2022

virus (POWV) (9), occurred in as early as the 1940s, surveillance and adequate diagnostic testing for these viruses continues to lag; however, the recent emergence and pandemic of Zika virus (ZIKV) suggests that renewed attention to these flaviviruses is warranted (10).

The Arboviral Diseases Branch, Division of Vector-Borne Diseases, Centers for Disease Control and Prevention maintains an inventory of over 500 arthropod-borne viruses and antigens for use in serodiagnostics, most of which are not available commercially (11). Viremia is brief and transient in most arboviral infections. Therefore, serodiagnosis is relied on for rapid detection of acute and convalescent infections. Standard serodiagnosis of flaviviruses includes enzyme-linked immunosorbent assays (ELISAs) for the detection of immunoglobulin M (IgM) or IgG, microsphere immunoassays (MIAs), or lateral flow assays for detection of antibody, while the plaque reduction neutralization test (PRNT) is used as the gold standard for confirmatory diagnosis. Immunoassays require the use of concentrated viral antigen, typically either using virus from infected cell culture supernatant or sucrose-acetone-extracted suckling mouse brain-derived antigen (12–14), both of which are laborious to produce and difficult to standardize in antigen production.

We previously developed gene cassettes to express virus-like particles (VLPs) consisting of flaviviral structural proteins, premembrane (prM), and envelope (E) in mammalian cell culture as an alternative to the typical viral-infected cell culture supernatant or suckling mouse brain-derived antigens (15). VLPs are antigenically similar to viruses but are noninfectious as they lack the genetic material to replicate while retaining the conformation of important immuno-dominant epitopes, allowing for use in serodiagnostics (16, 17). Within the last 20 years, flavivirus nonstructural protein 1 (NS1) has become an important marker for early diagnosis of acute flaviviral infections, including DENV, WNV, JEV, YFV, and ZIKV (18–27). To make antigen production faster and safer without the use of animals or hazardous chemicals, we previously developed stable COS-1 cell lines secreting VLPs for production of noninfectious flaviviral antigen to several medically important viruses, including WNV, DENV1-4, ZIKV, St. Louis encephalitis virus (SLEV), and JEV. However, we found that antigen secretion tended to wane over time in these cell lines, which has limited their usefulness (15, 28–30).

To overcome these difficulties with the COS-1 cell lines and to expand serology testing for diagnosis of emerging flaviviruses, we developed 39 stably expressing cell lines using human embryonic kidney-293 (HEK-293) cells expressing wild-type VLPs (WT-VLP), cross-reactive reduced VLPs (CRR-VLP), or antigenically modified VLPs with reduced cross-reactivity in the fusion peptide of the E protein and NS1 for 13 medically important or potentially emerging flaviviruses. We define medically important as flaviviruses known to cause human disease, while the emerging flaviviruses are defined as viruses with the potential to cause serious human disease. Flaviviruses included in the present study are DENV1 to DENV4, YFV, JEV, WNV, SLEV, ZIKV, ROCV, ILHV, USUV, and POWV. The HEK-293 cell line was chosen for its rapid growth and ability to produce large amounts of recombinant protein in a serum-free, chemically defined medium. HEK-293 cells have been used to generate stably secreting clones in many fields, including neuropharmacology, virology, and cell biology; however, most laboratories use the cell line for transient expression of recombinant proteins or use cell lines generated with selectable antibiotics (i.e., G418, zeocin, and hygromycin B) or through the use of inducible promoters (31–34).

Here, we report the clonal selection of these cell lines using no antibiotic selective pressure, and we demonstrate their superior abilities for sustained and improved production of recombinant viral antigens over previously developed COS-1 cell lines. Of the 39 stable HEK-293 cell lines generated, we observed that 35 of 39 cell lines (90%) exhibited stable expression of recombinant flaviviral antigen, 3 of 39 cell lines (7%) exhibited increased expression of recombinant flaviviral antigen, and only 1 of 39 cell lines (3%) exhibited decreased expression of recombinant flaviviral antigen. In direct comparison to nine previously developed COS-1 cell lines of the same constructs, all HEK-293 cell lines demonstrated higher antigen expression and secretion than several passages.

TABLE 1 Flaviviral VLP and NS1 gene cassette construct characteristics

Construct	Plasmid vector	Virus strain	Fusion loop mutations
DENV1 WT-VLP ^a	pVAX	Costa Rica 1994	
DENV1 CRR-VLP ^a			G106R/L107D
DENV1 NS1		16007	
DENV2 WT-VLP ^a	pVAX	16681	
DENV2 CRR-VLP ^a			G106R/L107K (30)
DENV2 NS1			
DENV3 WT-VLP ^a	pVAX	Panama 1994	
DENV3 CRR-VLP ^a			G106D/L107R (30)
DENV3 NS1			
DENV4 WT-VLP ^a	pCB	Honduras 1994	
DENV4 CRR-VLP ^a	pCB		G106E/L107D
DENV4 NS1	pVAX	Sri Lanka 1994	
ILHV WT-VLP ^a	pVAX	Original	
ILHV NS1		BRMSQ10	
JEV WT-VLP	pVAX	YL2009-4	
JEV CRR-VLP			G106K/L107D (66)
JEV NS1			
POWV WT-VLP	pVAX	LB	
POWV CRR-VLP			G106D
POWV NS1			
ROCV WT-VLP ^a	pVAX	SPH 34675	
ROCV CRR-VLP ^a			G106D/L107R
ROCV NS1			
SLEV WT-VLP	pVAX	MSI-7	
SLEV CRR-VLP			G106K/L107D (38)
SLE NS1			
USUV WT-VLP ^a	pVAX	Vienna 2001	
USUV CRR-VLP ^a			G106K/L107D
USUV NS1			
WNV WT-VLP	pVAX	NY99-6480	
WNV CRR-VLP	pCDNA3		G106R/L107H (36)
WNV NS1	pVAX		
YFV 17D WT-VLP	pCDNA3	17D	
YFV 17D CRR-VLP	pCDNA3		G106R/L107D
YFV 17D NS1	PVAX		
YFV IC WT-VLP	pCB	Ivory Coast 87	
ZIKV WT-VLP	pENTR	BPH2015	
ZIKV CRR-VLP			G106K/L107D (30)
ZIKV NS1	pVAX		

^aConstructs were composed of a chimeric gene cassette with 80% native E gene/20% JEV E gene.

RESULTS

Construction of gene cassettes for optimized expression of flaviviral antigen in HEK-293 cells. We aimed to develop stable cell lines expressing and secreting flaviviral VLPs and NS1 antigens using prM-E or NS1 gene constructs designed with the JEV signal sequence (JEVss) previously shown to enhance secretion of VLPs (16) (Table 1). While different plasmid vectors, including pCB, pCDNA3, and pVAX, were used throughout the construction process, no major differences between antigen expression and plasmid vector were observed. Sequences from current circulating viral strains were incorporated into the gene cassettes, otherwise, prototype viral strains were used

TABLE 2 ELISA and IFA results from a 4-day transient expression in HEK-293 cells with three different ILHV NS1 constructs

Construct	Reciprocal ELISA endpoint titer (log ₁₀)	IFA result ^a	Viral signal sequence
ILHV NS1	ND ^b	2%	JEV _{ss} (MGKRSASAGSIMWLASLAVVIAGTSA)
ILHV 2.6 NS1	1.9	60%	ILHV _{ss} (MLSVGGILLFLAVNVHA)
ILHV 3.8 NS1	2.5	80%	ILHV _{ss} (MGKMLSVGGILLFLAVNVHA)

^aRelative percentage of positive cells^bND, not detected.

for gene cassette construction (Table 1). The CRR-VLP constructs previously developed in COS-1 cells (DENV, WNV, SLEV, and JEV) were used to identify mutations in the fusion loop of the E protein (G106E/L107D, G106D/L107R, G106R/L107K, G106K/L107D, and G106R/L107H) that resulted in reduced binding of flavivirus group cross-reactive monoclonal antibodies 6B6C-1 and 4G2 (13, 35–38). Final mutations in the constructs were chosen based on highest immunofluorescence assay (IFA) expression, cell viability, and normal morphology and ELISA secretion after transient expression (Table 1). To increase antigen expression of some WT-VLPs and CRR-VLPs, we replaced the carboxy-terminal 20% of native virus E protein with the corresponding portion from JEV given that substitution with the JEV carboxy terminus was previously found to aid in secretion of DENV VLP constructs (Table 1) (39, 40).

Originally, the ILHV NS1 construct using the strain BrMS-MQ10 (NCBI accession number KC481679) (41) was designed with the JEV_{ss} preceding the NS1 gene similar to the other NS1 constructs; however, no secretion was observed during transient expression in HEK-293 cells. To increase efficiency of antigen secretion, two additional ILHV NS1 constructs were made with different signal peptides. ILHV 2.6 NS1 and ILHV 3.8 NS1 constructs, both of which used an internal ILHV signal sequence (ILHV_{ss}) located in the carboxy terminus of the envelope protein (17 amino acids of the carboxy terminus of E), were found to be more efficient with a signal peptide cleavage probability (Sec/SPI) of 0.94, while the JEV_{ss} had a Sec/SPI of 0.85, as calculated in SignalP-5.0 (42). Additionally, the ILHV 3.8 NS1 construct also included the amino acids glycine (G) and lysine (K) after the start codon of the ILHV_{ss} to increase the cleavage potential by the signal peptidase and subsequent antigen expression, which increased the signal peptide cleavage probability to 0.95 (43). Table 2 describes the antigen expression of these constructs from a 4-day transient expression. Only ILHV 2.6 NS1 and ILHV 3.8 NS1 had detectable antigen secretion by ELISA with reciprocal endpoint titers (EPT) of 1.9 and 2.5 log₁₀, respectively. While all constructs showed expression by IFA, only ILHV 2.6 NS1 and ILHV 3.8 NS1 had a relative percentage of positive NS1-expressing cells above 50% compared to the original ILHV NS1 construct, with 2% relative percent-positive NS1-expressing cells. Subsequently, the ILHV 3.8 NS1 construct was used for stable cell line development.

Development and evaluation of stable HEK-293 cell lines expressing flaviviral antigen. HEK-293 cells were transfected with selected plasmid constructs by electroporation, and cells were cloned in semisolid medium (3% carboxymethyl cellulose [CMC] mixed with HEK-293 growth medium) to isolate individual colonies. Throughout this period, clones were monitored for antigen production, and those with the highest antigen expression and secretion, as determined by ELISA, IFA, and cell viability, were retained. Clones were also selected based on normal cell morphology compared to normal HEK-293 cells. Cell lines with abnormal growth characteristics or morphology were abandoned. Clones with noticeable decreases in ELISA EPT or IFA expression were abandoned. We found that antigen secretion as measured by ELISA EPT and cell viability was better in a 1:1 mixture of two commercially available media, Expi-293 and Excell-293. The workflow for production and selection of stable cell lines producing recombinant flaviviral antigen is outlined in Fig. 1.

Thirty-five of 39 cell lines exhibited statistically stable EPTs by ELISA over 10 passages (Fig. 2). Cell lines DENV1 WT-VLP, DENV2 CRR-VLP, and YFV 17D WT-VLP exhibited statistically significant increasing antigen production over 10 passages with calculated slopes

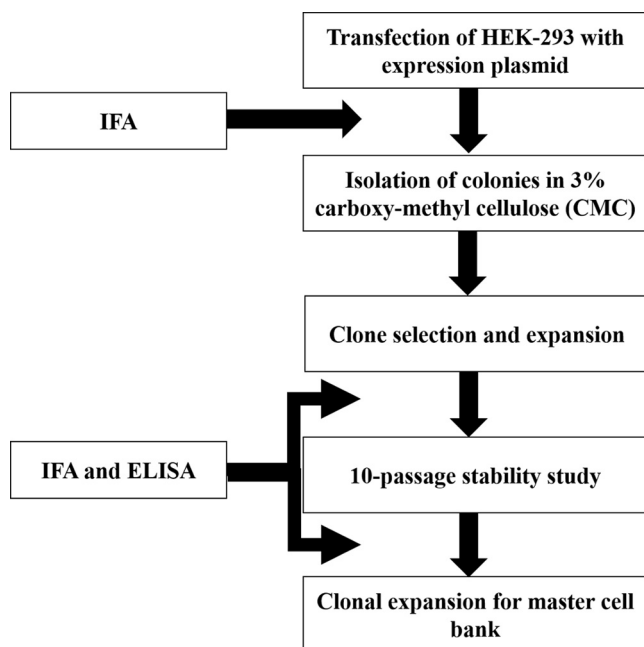


FIG 1 Workflow for production and selection of stable cell lines in the absence of selective pressure.

of 0.09, 0.33, and 0.25, respectively ($P < 0.05$; Fig. 2 and 3 and Table 3). DENV3 NS1 was the only cell line that exhibited statistically significant decreasing antigen production over 10 passages with a calculated slope of -0.27 ($P < 0.05$; Fig. 2 and 3 and Table 3). Cell lines with the highest mean EPT for each antigen type (WT-VLP, CRR-VLP, and NS1) were USUV WT-VLP, DENV3 CRR-VLP, and DENV4 NS1 (\log_2 [dilution] EPT of 11.83, 14.45, and 15.17, respectively; Fig. 2 and 3 and Table 4). Cell lines with the lowest mean EPT for each antigen type (WT-VLP, CRR-VLP, and NS1) were POW WT-VLP, POW CRR-VLP, and DENV3 NS1 (\log_2 [dilution] EPT of 1.17, 1.03, and 8.50, respectively; Fig. 2 and 3 and Table 4). NS1 cell lines produced more antigen than both the WT-VLP and CRR-VLP cell lines (9/13 cell lines), with consistently high amounts of antigen as seen by EPTs ranging from 8.5 to 15.17 (Fig. 2 and 3 and Table 4). Production of VLP antigen varied more widely among WT-VLP (range of EPTs of 1.17 to 11.83) and CRR-VLP cell lines (range of EPTs of 1.03 to 14.45). EPTs could not be calculated for ILHV WT-VLP, ROCV WT-VLP, and ROCV CRR-VLP due to the level of antigen being below the positive/negative (P/N) cutoff of 2.0. In a few cell lines (USUV WT-VLP, YF17D CRR-VLP, and DENV4 NS1), EPT could not be calculated for specific passages where the antigen was not titrated far enough to fall below the P/N cutoff of 2.0 (Fig. 2).

Comparison of flaviviral antigen produced in HEK-293 and COS-1 cell lines. To determine whether stable HEK-293 cell lines produced more recombinant antigen over several passages than previously derived COS-1 cell lines, nine antigen constructs, three each of WT-VLP, CRR-VLP, and NS1, were grown for 10 passages. Antigen expression and secretion were evaluated by ELISA, IFA, and flow cytometry (Fig. 4). Cell viability measured over 10 passages remained the same for both HEK-293 and COS-1 cells. All HEK-293 cell lines produced significantly higher quantities of recombinant flaviviral antigen (range of EPT of 5.23 to 14.45) than their COS-1 cell line counterparts (range of EPT of 1.33 to 6.50). The highest antigen-producing HEK-293 cell line was WNV NS1 (mean EPT of 14.25), and the highest producing COS-1 cell line was WNV CRR-VLP (mean EPT of 6.50). The lowest antigen-producing cell lines for both HEK-293 and COS-1 were DENV2 WT-VLP, with mean EPTs of 5.23 and 1.33, respectively. EPTs could not be calculated for some of the COS-1 cell lines, including DENV1 NS1, YFV WT-VLP, ZIKV NS1, and WNV NS1, given that recombinant antigen production was below the P/N cutoff of 2.0 while antigen was detectable for all HEK-293 cell lines in this comparison

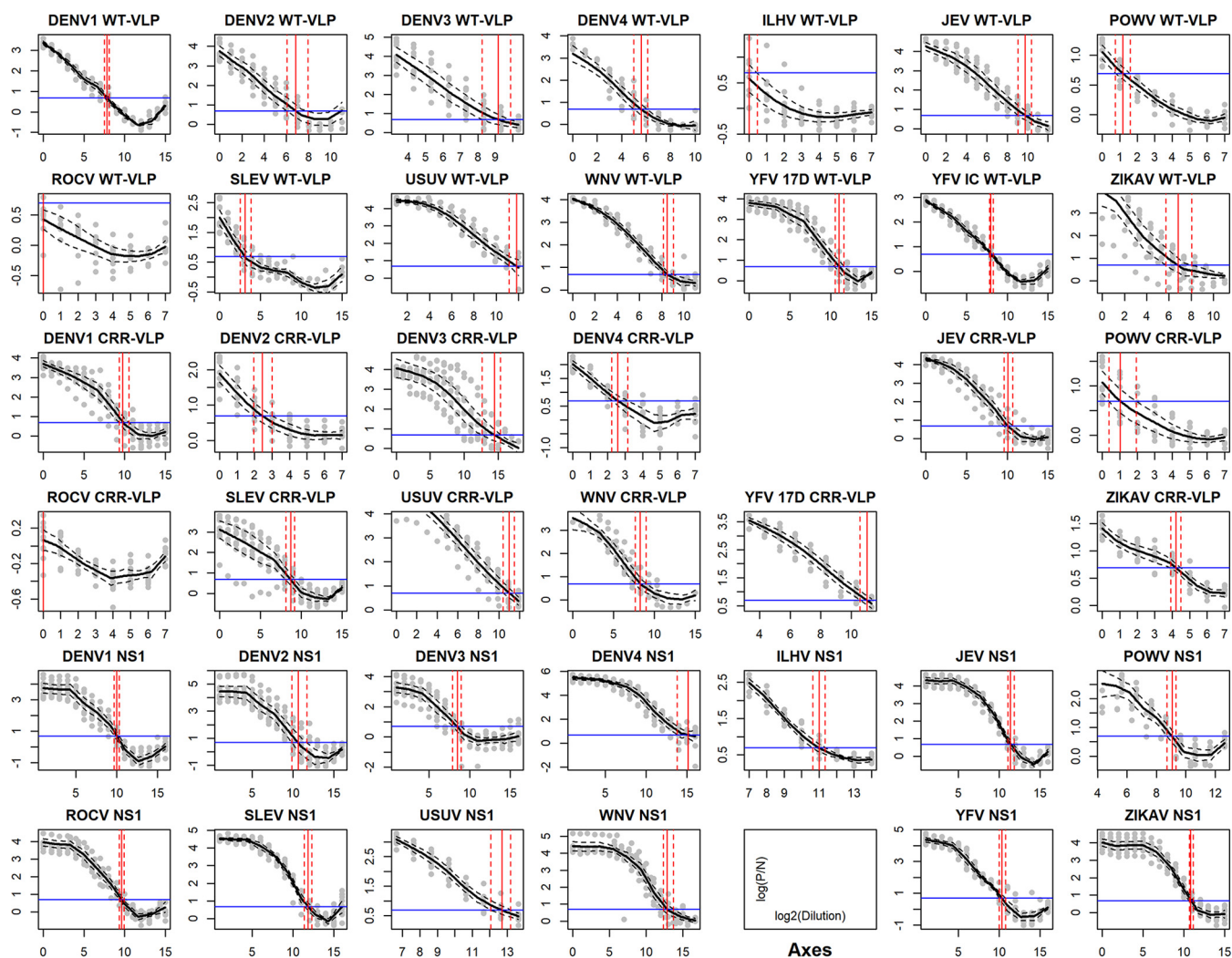


FIG 2 Predicted mean EPT curves over 10 passages for stable HEK-293 cell lines. Predicted mean values of EPTs (black line) from each cell line were plotted as $\log(P/N)$ versus \log_2 (dilution) with confidence bands shown as dashed black lines. P/N represents the ratio of the OD of positive antigen over the ratio of negative antigen tested in duplicate by ELISA. The reference line in blue for determining the EPT is shown at \log_2 . The estimated EPT (95% CI) is indicated with vertical red lines with confidence bands shown as dashed red lines.

experiment (Fig. 4 and Table 5). Similarly, HEK-293 cell lines were shown to have an increased relative percentage of positive intracellular expression of recombinant antigen at the 1st and 10th passages compared to COS-1 cell lines as measured by IFA (Fig. 5). Flow cytometry was used to quantitatively evaluate intracellular antigen expression over 10 passages for each cell line. Median percentages of positively expressing cells over 10 passages were compared for each recombinant antigen construct expressed in HEK-293 or COS-1 cell lines (Fig. 6). Intracellular antigen expression was significantly higher for the HEK-293 cell lines than for COS-1 cell lines for all cell lines evaluated, of which YFV 17D WT-VLP, WNV CRR-VLP, and WNV NS1 had median percent recombinant antigen expression above 95%. No COS-1 cell line had a median percent recombinant antigen expression above 25%. Taken together, these results demonstrate the sustained production of recombinant antigen in stable HEK-293 cells over several passages in culture as measured by ELISA, IFA, and flow cytometry and improvement of antigen production over the first generation of COS-1 cell lines.

DISCUSSION

This study reports on the development of a panel of cell lines stably expressing recombinant WT-VLP, CRR-VLP, and NS1 antigens for 13 medically important or potentially

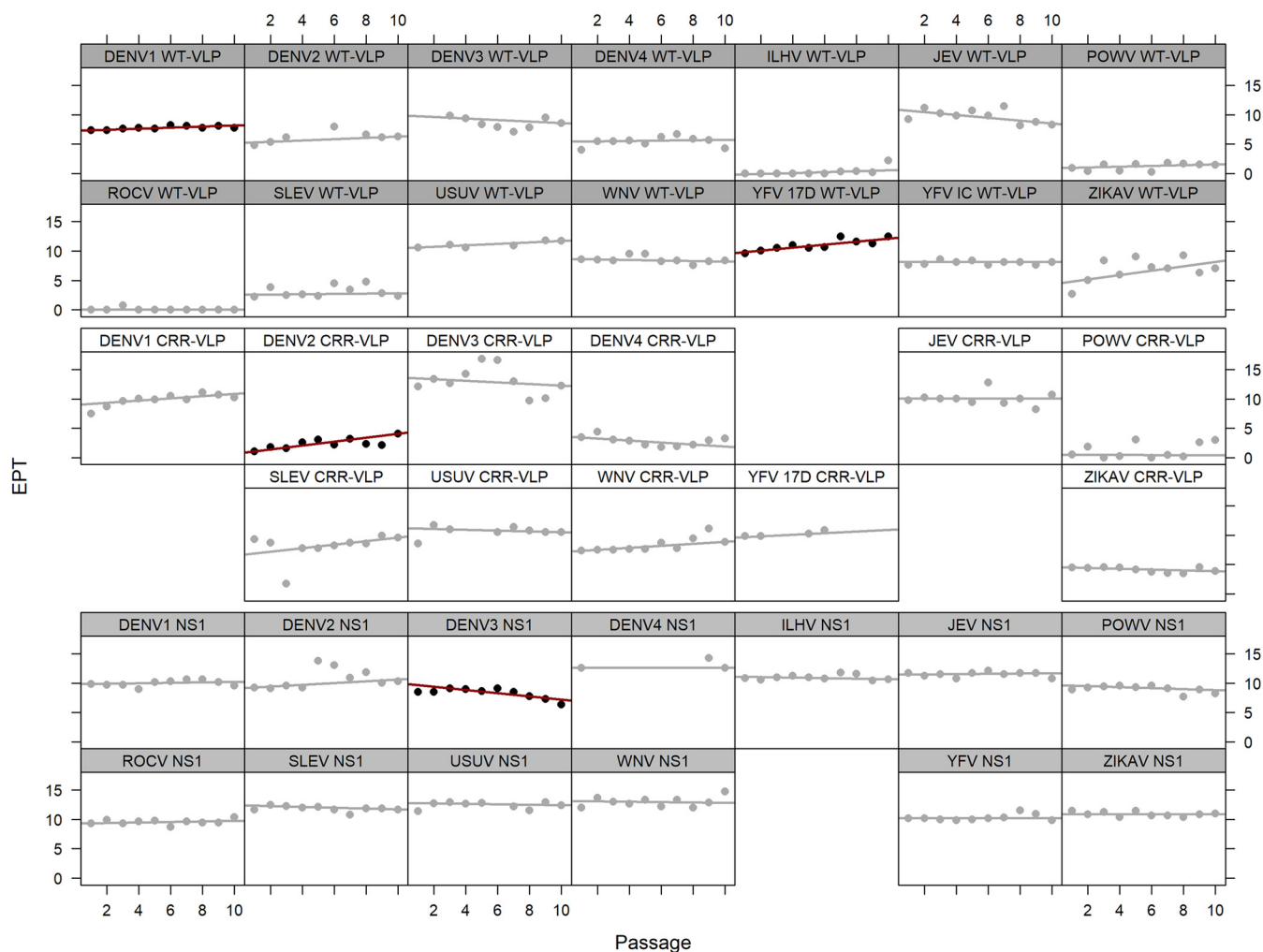


FIG 3 EPT against passage by cell line. Statistically significant trends ($P < 0.05$) are shown for the LAD regression test, with the fit drawn as a red line. Statistically nonsignificant LAD regression fits are shown as their corresponding regression lines in gray.

emerging flaviviruses. Four of 39 cell lines exhibited statistically increasing or decreasing trends of expression over 10 passages, with the remaining 35 cell lines exhibiting stable expression. Only one cell line (DENV3 NS1) was statistically shown to have decreasing antigen production over 10 passages, while three cell lines (DENV1 WT-VLP, DENV2 CRR-VLP, and YFV 17D WT-VLP) exhibited increased antigen production over 10 passages. For DENV1 WT-VLP, the slope of the plotted EPTs during 10 passages was lower (0.09) than the slopes of increasing EPTs for YFV 17D WT-VLP and DENV2 CRR-VLP (0.33 and 0.25, respectively), which had increased antigen production throughout cell passaging. Conversely, the slope of the plotted EPTs of DENV3 NS1 during 10 passages was -0.27 . This cell line had a relatively stable EPT from passages 1 to 6 before declining during passages 7 to 10. For the

TABLE 3 Estimated individual passage EPTs for cell lines with statistically significant LAD slopes

Cell line	Passage										95% CI ^a			
	1	2	3	4	5	6	7	8	9	10	Slope	Lower	Upper	P value ^b
DENV1 WT-VLP	7.35	7.35	7.65	7.80	7.65	8.26	8.11	7.80	8.11	7.80	0.09	0.00	0.13	0.02
DENV2 CRR-VLP	1.10	1.80	1.59	2.58	3.08	2.23	3.22	2.37	2.16	4.07	0.33	-0.05	0.33	0.01
YFV 17D WT-VLP	9.62	10.08	10.53	10.98	10.53	10.68	12.50	11.59	11.29	12.50	0.25	0.14	0.31	0.03
DENV3 NS1	8.50	8.50	9.11	8.95	8.65	9.11	8.50	7.74	7.29	6.38	-0.27	-0.36	0.01	0.02

^a95% confidence intervals (lower and upper limits).

^bP value for the test of slope = 0.

TABLE 4 Mean endpoint titers (95% CIs) by cell line over 10 passages

Cell line	EPT ^a	95% CI ^b	
		Lower	Upper
DENV1 WT-VLP	7.80	7.50	8.11
DENV1 CRR-VLP	9.77	9.32	10.53
DENV1 NS1	10.02	9.71	10.32
DENV2 WT-VLP	6.83	6.06	7.94
DENV2 CRR-VLP	2.44	1.94	3.01
DENV2 NS1	10.62	9.86	11.68
DENV3 WT-VLP	9.16	8.24	9.86
DENV3 CRR-VLP	14.45	12.64	15.36
DENV3 NS1	8.50	7.89	8.95
DENV4 WT-VLP	5.61	5.00	6.11
DENV4 CRR-VLP	2.58	2.23	3.15
DENV4 NS1	15.17	13.80	ND ^c
ILHV WT-VLP	ND ^c	ND ^c	0.46
ILHV NS1	10.99	10.64	11.35
JEV WT-VLP	9.76	9.03	10.36
JEV CRR-VLP	10.08	9.62	10.68
JEV NS1	11.38	11.08	11.83
POWV WT-VLP	1.17	0.74	1.59
POWV CRR-VLP	1.03	0.39	1.94
POWV NS1	9.07	8.74	9.32
ROCV WT-VLP	ND ^c	ND ^c	ND ^c
ROCV CRR-VLP	ND ^c	ND ^c	ND ^c
ROCV NS1	9.62	9.32	9.92
SLEV WT-VLP	3.11	2.50	3.86
SLEV CRR-VLP	8.71	8.11	9.17
SLEV NS1	11.83	11.38	12.29
USUV WT-VLP	11.83	11.17	ND ^c
USUV CRR-VLP	11.00	10.40	11.49
USUV NS1	12.69	12.05	13.18
WNV WT-VLP	8.50	8.17	9.06
WNV CRR-VLP	8.26	7.65	9.02
WNV NS1	12.86	12.36	13.70
YFV 17D WT-VLP	10.98	10.53	11.59
YFV IC WT-VLP	7.95	7.80	8.26
YFV 17D CRR-VLP	11.04	10.55	ND ^c
YFV 17D NS1	10.32	10.02	10.77
ZIKV WT-VLP	6.83	5.72	8.06
ZIKV CRR-VLP	4.21	3.92	4.49
ZIKV NS1	10.83	10.68	11.14

^aEPT recorded as log₂ (dilution).^b95% confidence interval (upper and lower).^cND, not determined.

ILHV WT-VLP, ROCV WT-VLP, and ROCV CRR-VLP cell lines, EPTs could not be calculated. However, in the case of ILHV and ROCV, we observed IFA expression throughout cell line development. Several reasons for this may exist. First, VLPs may have been trapped in the cell or the ELISA was suboptimal for detecting the VLPs. Second, the JEVs may have not been the ideal signal sequence to use in this situation, as was the case with ILHV NS1. Studies are ongoing to determine the reason for the low expression in these cell lines.

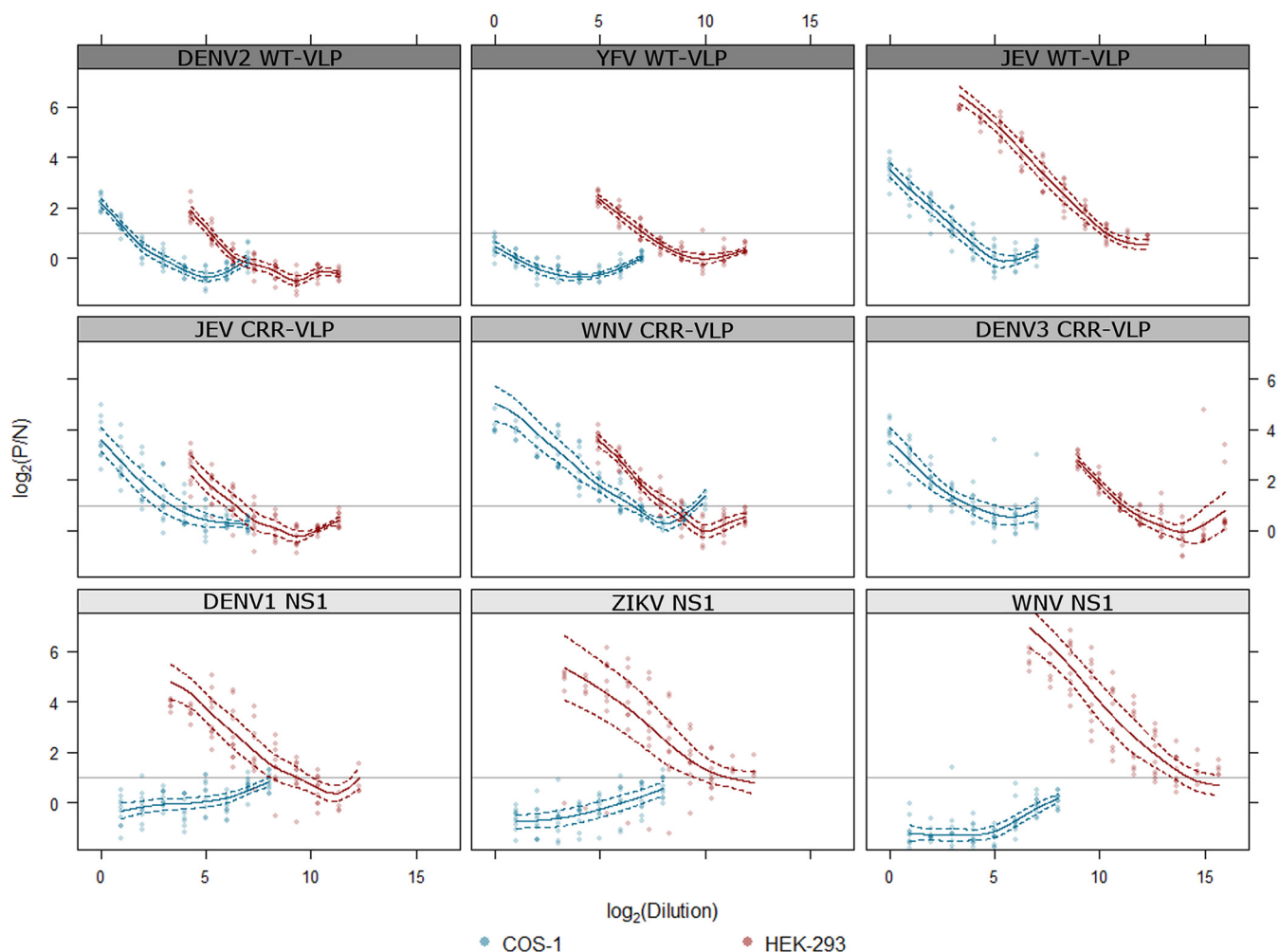


FIG 4 Comparison of antigen production from constitutively expressing flaviviral antigen COS-1 and HEK-293 cell lines. EPTs from antigen produced in COS-1 (blue) or HEK-293 (red) cell lines measured by ELISA were plotted as \log_2 (P/N) versus \log_2 (dilution), with confidence bands shown as dashed lines. P/N represents the ratio of the OD of positive antigen over the ratio of negative antigen tested in duplicate. The reference line shown in gray represents the P/N of 2 used to determine EPTs for each cell line.

Ninety percent of the cell lines developed in this project exhibited stable antigen expression over 10 passages. A few theories may point to the reason why we observed the changes in EPT in four cell lines. First, the cell lines with unstable EPTs may have been composed of producing and nonproducing cells, a phenomenon commonly seen

TABLE 5 Comparison of mean EPTs over 10 passages for selected COS-1 and HEK-293 cell lines constitutively expressing flaviviral recombinant antigen

Antigen ^a	EPT (95% CI) ^b	
	COS-1	HEK-293
DENV2 WT-VLP	1.33 (1.15 to 1.53)	5.23 (5.01 to 5.43)
JEV WT-VLP	3.38 (2.97 to 3.77)	10.33 (10.02 to 10.66)
YFV WT-VLP	ND ^c	7.08 (6.76 to 7.37)
DENV3 CRR-VLP	3.86 (3.23 to 5.06)	11.10 (10.85 to 11.40)
WNV CRR-VLP	6.50 (5.93 to 6.80)	8.19 (7.70 to 8.67)
JEV CRR-VLP	3.36 (2.50 to 4.14)	6.42 (5.85 to 6.93)
DENV1 NS1	ND ^c	9.34 (8.06 to 10.06)
WNV NS1	ND ^c	14.25 (13.44 to >14.65)
ZIKV NS1	ND ^c	11.07 (9.49 to >14.65)

^aRecombinant antigen from constitutively expressed cells.

^bEPTs and 95% CIs of antigen produced in COS-1 or HEK-293 cell lines and measured by ELISA.

^cND, not determined. EPT < 1.0 \log_2 (dilution).

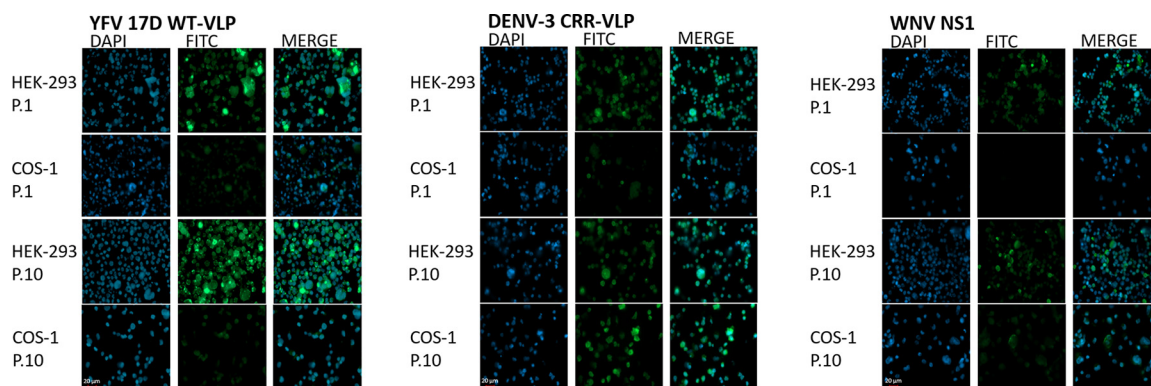


FIG 5 Intracellular expression of recombinant antigen from three representative HEK-293 and COS-1 VLP and NS1 constitutively expressing cell lines. Cells expressing recombinant antigen were harvested at the 1st and 10th passage, fixed, and stained with mouse hyperimmune ascitic fluid (MHIAF) and goat anti-mouse antibody conjugated to FITC. Nuclei of cells were stained with DAPI.

in hybridomas, which may arise due to changes in transcriptional capacity, mutations, loss of the gene of interest, or a combination of these factors (44). While the non-producing cells may have a growth advantage over the producing cells, they may not take over the entire population and can result in the diminished but not entire loss of recombinant antigen production (44–48). Second, cells within the population could lose copies of the recombinant gene, which may result in an overall decrease in recombinant antigen production (44, 49–51). Multiple copies of the expression vector may be introduced to the cell at the time of electroporation, and many of those copies may be maintained episomally or may randomly integrate into the host cell genome (44). If the gene of interest is integrated into the host cell genome, then this integration location may also play a role in the stability of recombinant antigen production (44, 52, 53). In cases where the integrated gene is in an advantageous location, we may see high recombinant antigen production, and in a disadvantageous location, we may see low recombinant antigen production (52, 53). Gene rearrangement or gene silencing could occur at any time the cell line is in culture, including during the 10-passage stability study, which may explain the increase or decrease in antigen production if the gene of interest were integrated in unstable locations in the cell genome (44).

The first iteration of stable cell lines developed in our lab for antigen production were in COS-1 cells. When HEK-293 and COS-1 cell lines using the same gene construct were compared, we found that all HEK-293 cell lines had higher antigen secretion than COS-1 cell lines. HEK-293 cell lines had higher percent viability as measured over 10 passages than COS-1 cells and grew at a higher density. For both HEK-293 and COS-1 cell lines, we noted no significant difference in cell viability or cell growth between antigen-expressing cells and normal cells. In the selection process for HEK-293 cell lines, we actively chose clones with growth characteristics similar to the normal HEK-293 cells (cell viability, morphology, and cell growth rate). Flow cytometry was introduced after all HEK-293 cell lines had been developed and was only used to evaluate the differences in recombinant antigen expression between COS-1 and HEK-293 cell lines. COS-1 cell lines were not developed using high recombinant protein expression measured by IFA as a primary selection criterion, which was included in the development of HEK-293 cell lines. This may explain the differences in flow cytometry median percentages of antigen-expressing cells and IFA expression between COS-1 and HEK-293 cell lines. Most HEK-293 cell lines expressed high levels of cell-associated recombinant antigen, as measured by flow cytometry, except DENV1 NS1, which showed 38% median percent recombinant antigen-positive cells. Conversely, all COS-1 cell lines expressed low levels of cell-associated recombinant antigen ($\leq 24\%$ positive cells). While we were constrained with the available COS-1 constructs to compare, the HEK-293 cell lines are an improvement over the first-generation COS-1 cell lines previously developed because of their stable constitutive expression of antigen.

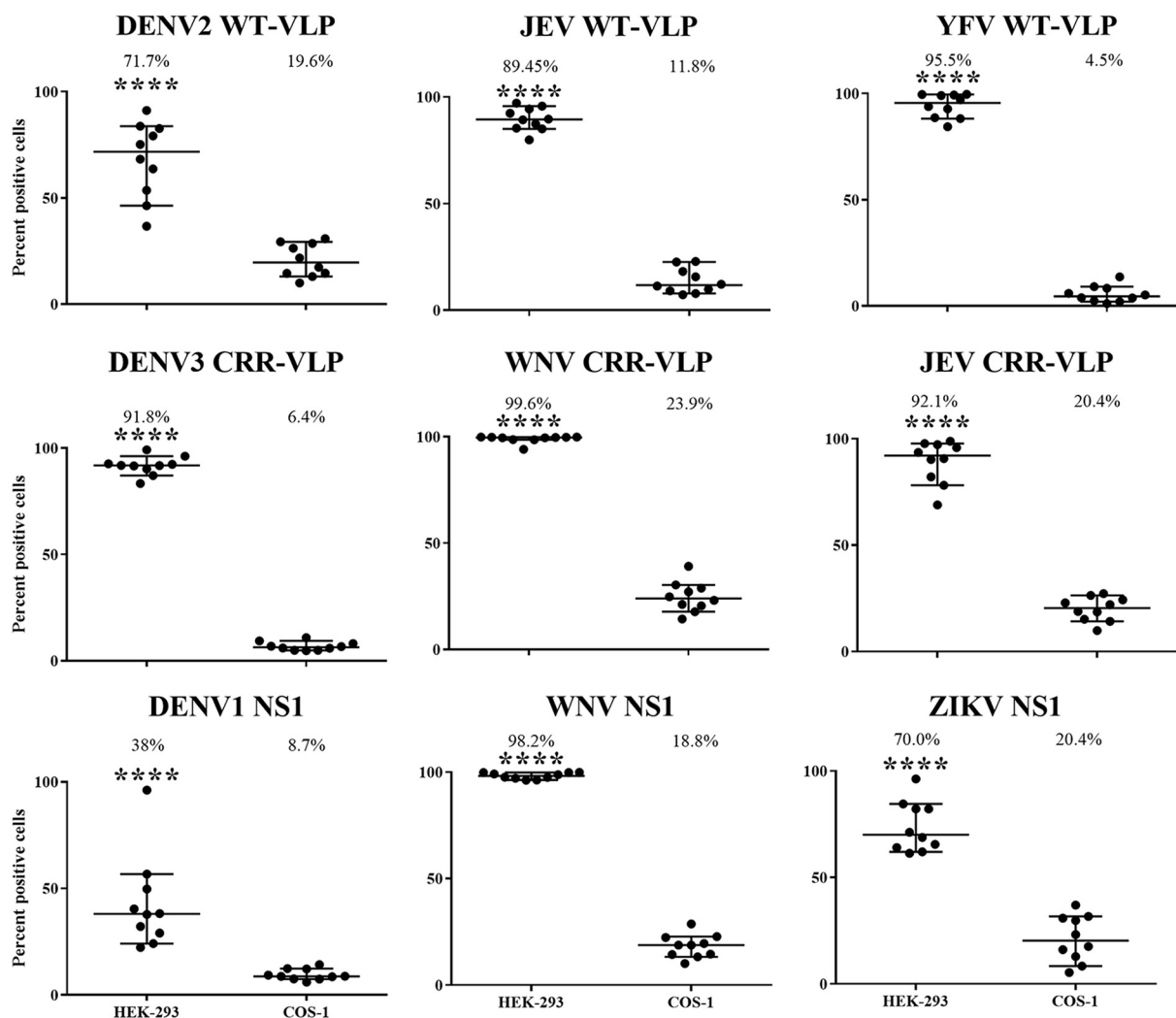


FIG 6 Recombinant antigen expression in HEK-293 and COS-1 cells was measured by flow cytometry over 10 passages. Significance in antigen expression between HEK-293 and COS-1 cell lines was measured by a two-tailed Mann-Whitney U test; ****, $P < 0.0001$. The median percent recombinant antigen expression (line and percentage) with 95% confidence interval is depicted for each cell line.

During cell line development, modifications of certain gene constructs were made to facilitate selection of the most efficient antigen-producing clones. We found that replacing 20% of the C terminus of the native viral envelope protein with the corresponding JEV envelope portion for several of the constructs enhanced expression and secretion of antigen in the newly developed HEK-293 cell lines (39, 40). Additionally, from previous work, we found that using the JEVss in recombinant constructs was an important factor in recombinant protein processing, cleavage, and secretion from transfected cells (16, 39, 40, 54). Thus, the JEVss was used in all constructs except ILHV NS1. In this case, we found that the native ILHV signal sequence had a more efficient signal peptide cleavage probability (Sec/SPI) than the cleavage probability of JEVss (42). Signal sequences may be influenced by the positively charged amino acids located in the N terminus of the peptide. Therefore, the addition of glycine (G) (neutral charge) and lysine (K) (positive charge) after the ILHV start codon was incorporated in the construct ILHV 3.8 NS1, which increased the signal peptide cleavage probability, resulted in higher ELISA EPT and IFA relative percent positivity.

To develop VLP antigens with low flavivirus group cross-reactivity for use in future serology assays aimed at flaviviral differential diagnosis, we incorporated mutations in the fusion peptide that were previously shown to ablate reactivity with flavivirus group cross-

reactive monoclonal antibodies (MAbs) (30, 35–38, 55, 56). Seminal work by Crill and Chang (2004) identified three amino acid residues in the fusion peptide (G104, G106, and L107) that are highly conserved among flaviviruses. Mutations at G106/L107 ablated reactivity with flavivirus group-reactive MAbs 4G2 and 6B6C-1 without loss of VLP secretion and production. However, mutations at G104, which lies in close proximity to the prM/M on the VLP, resulted in loss of particle secretion, which may have resulted in disruption of the prM/E interactions necessary for intracellular transport and secretion (35). Several of the G106 and L107 mutations in the flaviviral VLP have previously been incorporated in COS-1 cell line-produced antigen to improve differential diagnosis of SLEV/WNV and DENV/ZIKV infections by IgM antibody capture (MAC)-ELISA with promising results (30, 37, 56). Incorporation of these new HEK-293 CRR-VLPs together with NS1 antigens in serodiagnostic assays, such as MAC-ELISA and MIA, has the potential to enhance flaviviral differential diagnosis based on antibody reactivities from past and present infections.

Several modifications to the COS-1 cell line algorithm were made for the development of HEK-293 cell lines, which allowed for a more efficient and streamlined process. First, previously developed COS-1 cell lines were cloned by limiting dilution, which inherently results in a lower probability of obtaining the optimal clone as seeding cells and maintaining cultures at low density can be challenging (13, 15, 28, 29, 40). Conversely, HEK-293 cell lines were cloned in semisolid medium, which results in a much higher probability of clonality in the cell line once picked from the medium and better growth conditions for the cells. Coupled with automation of clone picking from the semisolid medium to 96-well plates, the clonal selection process for HEK-293 cell lines aided our ability to screen more clones.

Second, COS-1 cell lines were selected and grown under the constant presence of geneticin (G418) antibiotic throughout culture. While constitutively antigen-expressing COS-1 cells should be resistant to toxicity of G418 when expressing the G418 resistance gene within the plasmid, constant exposure to the antibiotic coupled with cells in culture for several months led to increased cell death with subsequent decreased recombinant protein production (13, 15, 28, 29, 40). HEK-293 cell lines were grown under no selective pressure, which provided a growth advantage throughout the selection process and subsequent passaging. Because antibiotics were not used for selection, between 800 and 2,400 clones from each cell line were screened to select clones with high reactivity in ELISA and IFA. Preliminary next-generation sequencing data suggest that for the HEK-293 cell lines sequenced, random integration of the expression plasmid and viral genes occurred in at least one chromosome of the host cell. Sequence analysis to determine plasmid integration loci is ongoing.

HEK-293 cell lines were selected based on antigen production by ELISA and cell-associated antigen expression by IFA, while COS-1 cell lines were only selected based on ELISA. We believe this aided our selection of final stable clones for the HEK-293 cell lines because we could observe changes in intracellular antigen expression by IFA coupled with ELISA EPT data to determine stability of clones. HEK-293 cells in our lab were found to grow exceptionally well, with a 4-day growth period resulting, on average, between 3- and 6-fold increases in cell density. The higher biomass that is achievable with suspension-grown cells results in more antigen production than that observed in adherent COS-1 cells that are inefficient in their requirement of high surface-to-volume ratio growth conditions (57). Last, HEK-293 cells are grown in serum-free, chemically defined medium, while COS-1 cells are grown in Dulbecco's modified Eagle medium (DMEM), with components such as fetal bovine serum (FBS) and additional supplements added prior to use. The HEK-293 cell culture medium has been specifically developed for this cell type, and we further optimized this medium for antigen secretion by using a 1:1 mixture of two commercially available HEK-293 media, which we found to increase recombinant antigen secretion, as seen in ELISA. The medium used for HEK-293 cells is serum free and chemically defined, and there were fewer lot to lot variations in medium as is seen with FBS-containing medium used for COS-1 cells. HEK-293 cells are NIH certified for use in biologics, which may allow for future use in vaccine development.

The HEK-293 cell lines constitutively expressing WT-VLPs, CRR-VLPs, and NS1 antigens for 13 medically important flaviviruses described herein provide a reproducible, safe, and superior source of antigen over traditional reagents and first-generation COS-1 recombinant cell lines. Like their predecessors, these cell lines, which include an expanded virus catalog of potentially emerging flaviviruses, will improve serodiagnostics with their ability to rapidly produce large quantities of antigen quickly and without the need for biocontainment. Additionally, the inclusion of WT-VLPs, CRR-VLPs, and NS1 for each flavivirus may facilitate future serodiagnostic algorithms for differential diagnosis of closely related flaviviruses. Future applications of this protocol include expansion to other high containment viruses, beginning with alphaviruses such as eastern equine encephalitis virus, western equine encephalitis virus, Venezuelan equine encephalitis virus, chikungunya virus, and Mayaro virus.

MATERIALS AND METHODS

Cell lines. Human embryonic kidney-293 cells (HEK-293; HEK-293.2sus CRL-1573.3, ATCC, VA, USA) were grown in a 1:1 mixture of Expi-293 medium (Thermo Fisher, MA, USA) and Ex-Cell medium (MilliporeSigma, MA, USA) with 1% (vol/vol) penicillin-streptomycin (Thermo Fisher, MA, USA). Cells were incubated at 37°C with 5% CO₂ in suspension with constant mixing at 130 rpm on orbital shaking platforms (Thermo Fisher, MA, USA). Seeding density for cells in culture were between 8×10^5 and 2×10^6 cells per mL (c/mL), and cells were subcultured every 3 to 4 days. Previously developed COS-1 cell lines expressing flaviviral antigen were cultured as previously described for comparison of antigen expression and production to stable HEK-293 cell lines (15, 16).

Viruses and antibodies. Stocks of flaviviruses, monoclonal antibodies (MAbs), virus-specific rabbit immune sera (RIS), and virus-specific mouse hyperimmune ascitic fluids (MHIAFs) were obtained from the Arbovirus Reference and Reagent Collection, Arbovirus Diagnostic Laboratory, Arbovirus Diseases Branch, Division of Vector-Borne Diseases, Centers for Disease Control and Prevention (Table S1 in the supplemental material). MAbs 6B6C-1 and 4G2, previously shown to be flavivirus group cross-reactive, were used to confirm lack of reactivity with CRR-VLP recombinant antigen in immunoassays (data not shown) (35, 58). MAbs 17BD3-2, 3.91D, D6-8A1-12, and Flo221 (a kind gift from Li-Kung Chen, College of Medicine, Tzu Chi University, Hualien, Taiwan) were purified as previously described and used in flow cytometry and IFA experiments (59–61).

Expression vectors. Expression vectors (pVAX, pcDNA3, pCB, and pENTR) were constructed with a Kozak consensus sequence (–9-GCCGCCGCatg+4) and the modified JEVs preceding the expression cassette (Table 1) (16). Restriction sites AfeI and NotI for prM-100%E or AfeI and StuI for prM-80% native E gene/20% JEV E gene (New England Biolabs, MA, USA) were used to insert the gene of interest into the expression vector.

Gene cassette composition and synthesis. Flavivirus VLPs composed of the structural genes prM and E and NS1 constructs were developed as previously described (15, 28). WT-VLP constructs possessed intact genetic sequence, while CRR-VLP constructs contained two mutations at amino acid residues 106 and 107 in the fusion peptide of the E protein (35). CRR-VLP constructs were made using site-directed mutagenesis as previously described (35). While half of the VLP gene cassettes contained 100% of their native E gene, the other half contained only 80% of their native E gene, and 20% of JEV carboxy-terminal E (Table 1) (39). Expression vectors containing the gene cassettes were produced in *Escherichia coli* (NEB Express high-efficiency *E. coli* sequence C2523H; NEB, MA, USA) using manufacturer's growth conditions, plasmid DNA extraction, and sequence confirmation protocols as previously described (16).

Transfection of HEK-293 cells. HEK-293 cells were electroporated with expression vectors containing the gene cassettes as previously described with the following modifications (16). Plasmid DNA (30 μg per reaction) was added to 0.5 mL of cells (cell density equal to 1 to 2.0×10^7 cells/mL) and placed into a cuvette with a 4-mm gap (Bio-Rad, CA, USA). A GenePulser Xcell (Bio-Rad, CA, USA) was used with the following settings: voltage of 250 V, capacitance of 975 μF, and resistance of ∞ (infinity). Electroporated cells were recovered in medium and seeded at a final density of 2.5×10^6 to 5×10^6 c/mL and grown overnight at 37°C with 5% CO₂. For transient expression, transfected cells were grown for 1 to 4 days without changing the medium. After transient expression was complete, supernatant was collected by centrifugation, and cells were discarded.

Immunofluorescence. Immunofluorescence assays (IFAs) were used to evaluate expression of cell-associated antigen as previously described with some modifications (16). Briefly, cells were harvested, dried onto 12-well or 15-well glass slides (MP Biomedicals, CA, USA), and fixed with cold 3:1 (vol/vol) acetone-phosphate-buffered saline (PBS; stored at –20°C) for 10 min. Cells were stained with virus-specific MHIAF (1:200, diluted in PBS) for 30 min before being washed with PBS and then stained with goat anti-mouse fluorescein isothiocyanate (FITC)-conjugated antibody (1:100, diluted in PBS; Jackson ImmunoResearch, PA, USA). Slides were washed and mounted with Prolong Diamond Antifade Mountant with 4',6-diamidino-2-phenylindole (DAPI; Thermo Fisher, MA, USA) with a coverslip and incubated for 24 h at room temperature before being examined on an epifluorescence microscope (Zeiss, Germany).

Flow cytometry. Cells were grown under standard culture conditions prior to fixation. Following the manufacturer's protocol, 1×10^7 cells were fixed using 4% paraformaldehyde for 20 min at 4°C followed by two washes in sterile, cold $1 \times$ PBS (BD Biosciences, CA, USA). Cells were frozen in 90% FBS/10% dimethyl sulfoxide (DMSO) and stored at –80°C before proceeding. Once cells were thawed, they were

washed twice with magnetically activated cell sorting (MACS) buffer (Miltenyi Biotec, Germany) to remove DMSO and permeabilized with BD PermWash (BD Biosciences, CA, USA) according to the manufacturer's protocol. After permeabilization, cells were blocked with 1% bovine serum albumin (BSA; Millipore, IL, USA) in PBS for 30 min at 4°C with agitation. MAbs (10 µg/mL) were diluted in blocking buffer and incubated at 4°C for 30 min with agitation. R-Phycoerythrin AffiniPure goat anti-mouse IgG (H+L; Jackson ImmunoResearch, PA, USA) was diluted in blocking buffer and incubated with cells for 30 min at 4°C with agitation. Cells were resuspended in 200 µL of MACS buffer prior to reading on a BD Accuri C6 flow cytometer (BD Biosciences, NJ, USA). Data analysis was performed in FlowJo (version 10, BD Biosciences, NJ, USA). Significance in antigen expression between HEK-293 and COS-1 cell lines was measured by a two-tailed Mann-Whitney U test in GraphPad Prism 6.0.

Antigen capture ELISA. Antigen capture ELISA was performed as previously described with some modifications (15, 16). Rabbit immune sera raised against the homologous virus was used as capture antibody. Immulon II plates (VWR, PA, USA) were coated in carbonate-bicarbonate buffer (50 mM sodium carbonate, 50 mM sodium bicarbonate, pH 9.6; Thermo Fisher, MA, USA) and incubated overnight at 4°C. Nonspecific binding sites were blocked with StartingBlock (200 µL/well; Thermo Fisher, MA, USA) before cell culture supernatant was added to the plates (50 µL/well) and incubated for 2 h at 37°C, after which plates were washed five times with PBS/0.1% Tween wash buffer with an automatic plate washer. Virus-specific MHIAF diluted in PBS was mixed with 5% nonfat dry milk (Thermo Fisher, MA, USA) in PBS (50 µL/well) and was incubated on the plate for 1 h at 37°C. Plates were washed again, and peroxidase-conjugated goat anti-mouse antibody (Jackson ImmunoResearch, PA, USA) diluted 1:8,000 in 5% nonfat milk/PBS (50 µL/well) was incubated at 37°C for 1 h. After a final wash, 3,3',5,5'-tetramethylbenzidine (TMB) substrate (KPL, MA, USA) was added (100 µL/well) and incubated for 10 min at room temperature. The reaction was stopped with 2 N H₂SO₄ (50 µL/well; VWR, PA, USA), and optical density (OD) was measured as a ratio of 450/630 nm.

Indirect ELISA. NS1 antigen from cell culture supernatant was coated directly to the Immulon II plate in doubling dilutions starting with 1:2 in carbonate-bicarbonate buffer, and plates were incubated at 4°C overnight. The rest of the procedure was performed as described above.

Stable cell line development. After antigen expression was confirmed by IFA (≥20%) the day after electroporation, cells were seeded at a density of 2×10^5 to 2×10^6 c/mL in 3% CMC (medium viscosity; Millipore Sigma, MA, USA) resuspended with HEK-293 cell culture medium, and cells were cultured for 7 to 14 days at 37°C with 5% CO₂. Colonies were identified and selected using the ClonePix2 automated mammalian colony picker (Molecular Devices, CA, USA) according to the manufacturer's instructions. Cells were picked by the ClonePix2 from the CMC and placed in a 96-well plate prefilled with 150 µL of cell culture medium (Corning, NY, USA). Cloned cells were grown in 96-well plates to 50 to 100% confluency (approximately 7 to 14 days) before being screened by ELISA and IFA. Up to 50 clones were passed into 24-well plates and selected thereafter (Fig. 1).

Statistical analysis. To determine whether the constitutively expressing cell lines produced antigen consistently over several passages, cell lines were passaged 10 times, and cell culture supernatants from each passage were evaluated by ELISA. To determine any potential systematic change in antigen production over the passages, we first calculated the estimated endpoint titer (EPT) based on each passage within each cell line. The EPT was defined as the lowest dilution that results in a positive/negative (P/N) ratio of 2. Positive/negative ratios were determined by taking the average OD of supernatant from the test antigen divided by the average OD of the supernatant from normal HEK-293 cells. In the case that the observed data points for a single passage did not measure below a P/N of 2, the EPT was not estimated. Fig. 2 shows the individual predicted mean curves (95% pointwise confidence intervals [CIs]) for each passage and cell line (62). The EPTs estimated using the mean curves (95% CIs) shown in Fig. 2 are listed in Table 4. Next, the EPTs of each passage within each cell line were subsequently analyzed using least absolute deviation (LAD) regression to evaluate the slope of the regression line of EPT against passage sequence number.

Semiparametric, penalized regression was used to model log (P/N) as a smooth function of log₂ (dilution), where different passage curves were considered random observations about a theoretical mean curve (63). Individual and mean curves and corresponding 95% confidence intervals were estimated using the code and methods of Heckman et al. (2013) (62). EPTs (95% CIs) were estimated from these fitted curves as the point at which they crossed log (2). Once computed, the EPTs were modeled as a linear function of passage sequence number, with the linear model parameter intercept and slope estimated using LAD regression. To evaluate linear trend in EPT by passage, we tested the hypothesis that the slope was 0 using the standard analysis of variance (ANOVA) test for ordinary least squares (OLS) regression and the Wald test, following the recommendation in Bassett and Koenker (64). Analyses were performed in the R software package (65).

SUPPLEMENTAL MATERIAL

Supplemental material is available online only.

SUPPLEMENTAL FILE 1, PDF file, 0.1 MB.

ACKNOWLEDGMENTS

Financial support for J.A.P., B.S.D., L.R., and E.G. and the work presented here was provided to G.-J.C. by an interagency agreement with BARDA (IAA750117PR09000036). W.M.S. acknowledges support from the Global Virus Network Fellowship and was supported by São Paulo Research Foundation #2017/13981-0. M.J.F. was supported by São Paulo

Research Foundation #2018/09383-3. This project was supported, in part, by an appointment to the Research Participation Program at the Centers for Disease Control and Prevention administered by the Oak Ridge Institute for Science and Education through an interagency agreement between the U.S. Department of Energy and the Centers for Disease Control and Prevention.

We thank Li-Kung Chen, College of Medicine, Tzu Chi University, Hualien, Taiwan, for the MAb Flo221. We appreciate John Lee, BARDA project officer, and William Kramp for their lively discussion and constant encouragement.

The findings and conclusions in this report are those of the authors and do not necessarily represent the official position of the CDC.

REFERENCES

- Kraemer MUG, Reiner RC Jr, Brady OJ, Messina JP, Gilbert M, Pigott DM, Yi D, Johnson K, Earl L, Marczak LB, Shirude S, Davis Weaver N, Bisanzio D, Perkins TA, Lai S, Lu X, Jones P, Coelho GE, Carvalho RG, Van Bortel W, Marsboom C, Hendrickx G, Schaffner F, Moore CG, Nax HH, Bengtsson L, Wetter E, Tatem AJ, Brownstein JS, Smith DL, Lambrechts L, Cauchemez S, Linard C, Faria NR, Pybus OG, Scott TW, Liu Q, Yu H, Wint GRW, Hay SI, Golding N. 2019. Past and future spread of the arbovirus vectors *Aedes aegypti* and *Aedes albopictus*. *Nat Microbiol* 4:854–863. <https://doi.org/10.1038/s41564-019-0376-y>.
- Bhatt S, Gething PW, Brady OJ, Messina JP, Farlow AW, Moyes CL, Drake JM, Brownstein JS, Hoen AG, Sankoh O, Myers MF, George DB, Jaenisch T, Wint GR, Simmons CP, Scott TW, Farrar JJ, Hay SI. 2013. The global distribution and burden of dengue. *Nature* 496:504–507. <https://doi.org/10.1038/nature12060>.
- Messina JP, Brady OJ, Golding N, Kraemer MUG, Wint GRW, Ray SE, Pigott DM, Shearer FM, Johnson K, Earl L, Marczak LB, Shirude S, Davis Weaver N, Gilbert M, Velayudhan R, Jones P, Jaenisch T, Scott TW, Reiner RC Jr, Hay SI. 2019. The current and future global distribution and population at risk of dengue. *Nat Microbiol* 4:1508–1515. <https://doi.org/10.1038/s41564-019-0476-8>.
- Monath TP, Vasconcelos PF. 2015. Yellow fever. *J Clin Virol* 64:160–173. <https://doi.org/10.1016/j.jcv.2014.08.030>.
- Schuh AJ, Ward MJ, Leigh Brown AJ, Barrett AD. 2014. Dynamics of the emergence and establishment of a newly dominant genotype of Japanese encephalitis virus throughout Asia. *J Virol* 88:4522–4532. <https://doi.org/10.1128/JVI.02686-13>.
- Roesch F, Fajardo A, Moratorio G, Vignuzzi M. 2019. Usutu virus: an arbovirus on the rise. *Viruses* 11:640. <https://doi.org/10.3390/v11070640>.
- Saivish MV, da Costa VG, Rodrigues RL, Feres VCR, Montoya-Diaz E, Moreli ML. 2020. Detection of Rocio virus SPH 34675 during dengue epidemics, Brazil, 2011–2013. *Emerg Infect Dis* 26:797–799. <https://doi.org/10.3201/2604.190487>.
- Cunha MS, Luchs A, da Costa AC, Ribeiro GO, Dos Santos FCP, Nogueira JS, Komninakis SV, Marinho RDSS, Witkin SS, Villanova F, Deng X, Sabino EC, Delwart E, Leal E, Nogueira ML, Maiorka PC. 2020. Detection and characterization of Ilheus and Iguape virus genomes in historical mosquito samples from Southern Brazil. *Acta Trop* 205:105401. <https://doi.org/10.1016/j.actatropica.2020.105401>.
- Hernance ME, Thangamani S. 2017. Powassan virus: an emerging arbovirus of public health concern in North America. *Vector Borne Zoonotic Dis* 17:453–462. <https://doi.org/10.1089/vbz.2017.2110>.
- Pierson TC, Diamond MS. 2020. The continued threat of emerging flaviviruses. *Nat Microbiol* 5:796–812. <https://doi.org/10.1038/s41564-020-0714-0>.
- Centers for Disease Control and Prevention. 2022. Division of Vector-Borne Diseases Arbovirus Reference Collection. <https://www.cdc.gov/ncezid/dvbd/specimensub/arc/index.html>. Accessed April 22, 2022.
- Curren EJ, Venkat H, Sunenshine R, Fitzpatrick K, Kosoy O, Krow-Lucal E, Zabel K, Adams L, Kretschmer M, Fischer M, Hills SL. 2020. Assessment of immunoglobulin M enzyme-linked immunosorbent assay ratios to identify West Nile virus and St. Louis encephalitis virus infections during concurrent outbreaks of West Nile virus and St. Louis encephalitis virus diseases, Arizona 2015. *Vector Borne Zoonotic Dis* 20:619–623. <https://doi.org/10.1089/vbz.2019.2571>.
- Holmes DA, Purdy DE, Chao DY, Noga AJ, Chang GJ. 2005. Comparative analysis of immunoglobulin M (IgM) capture enzyme-linked immunosorbent assay using virus-like particles or virus-infected mouse brain antigens to detect IgM antibody in sera from patients with evident flaviviral infections. *J Clin Microbiol* 43:3227–3236. <https://doi.org/10.1128/JCM.43.7.3227-3236.2005>.
- Kuno G. 2003. Serodiagnosis of flaviviral infections and vaccinations in humans. *Adv Virus Res* 61:3–65. [https://doi.org/10.1016/s0065-3527\(03\)61001-8](https://doi.org/10.1016/s0065-3527(03)61001-8).
- Hunt AR, Cropp CB, Chang G-JJ. 2001. A recombinant particulate antigen of Japanese encephalitis virus produced in stably-transformed cells is an effective noninfectious antigen and subunit immunogen. *J Virol Methods* 97:133–149. [https://doi.org/10.1016/S0166-0934\(01\)00346-9](https://doi.org/10.1016/S0166-0934(01)00346-9).
- Chang GJ, Hunt AR, Davis B. 2000. A single intramuscular injection of recombinant plasmid DNA induces protective immunity and prevents Japanese encephalitis in mice. *J Virol* 74:4244–4252. <https://doi.org/10.1128/jvi.74.9.4244-4252.2000>.
- Heinz FX, Stiasny K. 2017. The antigenic structure of Zika virus and its relation to other flaviviruses: implications for infection and immunoprophylaxis. *Microbiol Mol Biol Rev* 81:e00055-16. <https://doi.org/10.1128/MMBR.00055-16>.
- Chao D-Y, Galula JU, Shen W-F, Davis BS, Chang G-JJ. 2015. Nonstructural protein 1-specific immunoglobulin M and G antibody capture enzyme-linked immunosorbent assays in diagnosis of flaviviral infections in humans. *J Clin Microbiol* 53:557–566. <https://doi.org/10.1128/JCM.02735-14>.
- Huang JL, Huang JH, Shyu RH, Teng CW, Lin YL, Kuo MD, Yao CW, Shaio MF. 2001. High-level expression of recombinant dengue viral NS-1 protein and its potential use as a diagnostic antigen. *J Med Virol* 65:553–560. <https://doi.org/10.1002/jmv.2072>.
- Musso D, Despres P. 2020. Serological diagnosis of flavivirus-associated human infections. *Diagnostics (Basel)* 10:302. <https://doi.org/10.3390/diagnostics10050302>.
- Jaaskelainen AJ, Korhonen EM, Huhtamo E, Lappalainen M, Vapalahti O, Kallio-Kokko H. 2019. Validation of serological and molecular methods for diagnosis of Zika virus infections. *J Virol Methods* 263:68–74. <https://doi.org/10.1016/j.jviromet.2018.10.011>.
- Lima MdRQ, Nogueira RMR, Schatzmayr HG, de Santos FB. 2010. Comparison of three commercially available dengue NS1 antigen capture assays for acute diagnosis of dengue in Brazil. *PLoS Negl Trop Dis* 4:e738. <https://doi.org/10.1371/journal.pntd.0000738>.
- Ricciardi-Jorge T, Bordignon J, Koishi A, Zanluca C, Mosimann AL, Duarte Dos Santos CN. 2017. Development of a quantitative NS1-capture enzyme-linked immunosorbent assay for early detection of yellow fever virus infection. *Sci Rep* 7:16229. <https://doi.org/10.1038/s41598-017-16231-6>.
- Macdonald J, Tonry J, Hall RA, Williams B, Palacios G, Ashok MS, Jabado O, Clark D, Tesh RB, Briese T, Lipkin WI. 2005. NS1 protein secretion during the acute phase of West Nile virus infection. *J Virol* 79:13924–13933. <https://doi.org/10.1128/JVI.79.22.13924-13933.2005>.
- Young PR, Hilditch PA, Bletchly C, Halloran W. 2000. An antigen capture enzyme-linked immunosorbent assay reveals high levels of the dengue virus protein NS1 in the sera of infected patients. *J Clin Microbiol* 38:1053–1057. <https://doi.org/10.1128/JCM.38.3.1053-1057.2000>.
- Kumar JS, Parida M, Rao PV. 2011. Monoclonal antibody-based antigen capture immunoassay for detection of circulating non-structural protein NS1: implications for early diagnosis of Japanese encephalitis virus infection. *J Med Virol* 83:1063–1070. <https://doi.org/10.1002/jmv.22097>.
- Chung KM, Diamond MS. 2008. Defining the levels of secreted non-structural protein NS1 after West Nile virus infection in cell culture and mice. *J Med Virol* 80:547–556. <https://doi.org/10.1002/jmv.21091>.

28. Davis BS, Chang GJ, Cropp B, Roehrig JT, Martin DA, Mitchell CJ, Bowen R, Bunning ML. 2001. West Nile virus recombinant DNA vaccine protects mouse and horse from virus challenge and expresses *in vitro* a noninfectious recombinant antigen that can be used in enzyme-linked immunosorbent assays. *J Virol* 75:4040–4047. <https://doi.org/10.1128/JVI.75.9.4040-4047.2001>.
29. Purdy DE, Noga AJ, Chang GJ. 2004. Noninfectious recombinant antigen for detection of St. Louis encephalitis virus-specific antibodies in serum by enzyme-linked immunosorbent assay. *J Clin Microbiol* 42:4709–4717. <https://doi.org/10.1128/JCM.42.10.4709-4717.2004>.
30. Chao DY, Whitney MT, Davis BS, Medina FA, Munoz JL, Chang GJ. 2019. Comprehensive evaluation of differential serodiagnosis between Zika and dengue viral infections. *J Clin Microbiol* 57:e01506-18. <https://doi.org/10.1128/JCM.01506-18>.
31. Thomas P, Smart TG. 2005. HEK293 cell line: a vehicle for the expression of recombinant proteins. *J Pharmacol Toxicol Methods* 51:187–200. <https://doi.org/10.1016/j.vascn.2004.08.014>.
32. Venereo-Sanchez A, Simoneau M, Lanthier S, Chahal P, Bourget L, Ansoerge S, Gilbert R, Henry O, Kamen A. 2017. Process intensification for high yield production of influenza H1N1 Gag virus-like particles using an inducible HEK-293 stable cell line. *Vaccine* 35:4220–4228. <https://doi.org/10.1016/j.vaccine.2017.06.024>.
33. Bora RS, Gupta D, Malik R, Chachra S, Sharma P, Saini KS. 2008. Development of a cell-based assay for screening of phosphodiesterase 10A (PDE10A) inhibitors using a stable recombinant HEK-293 cell line expressing high levels of PDE10A. *Biotechnol Appl Biochem* 49:129–134. <https://doi.org/10.1042/BA20070090>.
34. Bussow K. 2015. Stable mammalian producer cell lines for structural biology. *Curr Opin Struct Biol* 32:81–90. <https://doi.org/10.1016/j.sbi.2015.03.002>.
35. Crill WD, Chang GJ. 2004. Localization and characterization of flavivirus envelope glycoprotein cross-reactive epitopes. *J Virol* 78:13975–13986. <https://doi.org/10.1128/JVI.78.24.13975-13986.2004>.
36. Crill WD, Trainor NB, Chang G-JJ. 2007. A detailed mutagenesis study of flavivirus cross-reactive epitopes using West Nile virus-like particles. *J Gen Virol* 88:1169–1174. <https://doi.org/10.1099/vir.0.82640-0>.
37. Roberson JA, Crill WD, Chang G-JJ. 2007. Differentiation of West Nile and St. Louis encephalitis virus infections by use of noninfectious virus-like particles with reduced cross-reactivity. *J Clin Microbiol* 45:3167–3174. <https://doi.org/10.1128/JCM.01143-07>.
38. Trainor NB, Crill WD, Roberson JA, Chang G-JJ. 2007. Mutation analysis of the fusion domain region of St. Louis encephalitis virus envelope protein. *Virology* 360:398–406. <https://doi.org/10.1016/j.virol.2006.10.033>.
39. Chang G-JJ, Hunt AR, Holmes DA, Springfield T, Chieh TS, Roehrig JT, Gubler DJ. 2003. Enhancing biosynthesis and secretion of premembrane and envelope proteins by the chimeric plasmid of dengue virus type 2 and Japanese encephalitis virus. *Virology* 306:170–180. [https://doi.org/10.1016/s0042-6822\(02\)00028-4](https://doi.org/10.1016/s0042-6822(02)00028-4).
40. Purdy DE, Chang GJ. 2005. Secretion of noninfectious dengue virus-like particles and identification of amino acids in the stem region involved in intracellular retention of envelope protein. *Virology* 333:239–250. <https://doi.org/10.1016/j.virol.2004.12.036>.
41. Pauvolid-Correa A, Kenney JL, Couto-Lima D, Campos ZM, Schatzmayr HG, Nogueira RMR, Brault AC, Komar N. 2013. Ilheus virus isolation in the Pantanal, west-central Brazil. *PLoS Negl Trop Dis* 7:e2318. <https://doi.org/10.1371/journal.pntd.0002318>.
42. Almagro Armenteros JJ, Tsirigos KD, Sonderby CK, Petersen TN, Winther O, Brunak S, von Heijne G, Nielsen H. 2019. SignalP 5.0 improves signal peptide predictions using deep neural networks. *Nat Biotechnol* 37:420–423. <https://doi.org/10.1038/s41587-019-0036-z>.
43. Chang GJ, Davis BS, Hunt AR, Holmes DA, Kuno G. 2001. Flavivirus DNA vaccines: current status and potential. *Ann N Y Acad Sci* 951:272–285.
44. Barnes LM, Bentley CM, Dickson AJ. 2003. Stability of protein production from recombinant mammalian cells. *Biotechnol Bioeng* 81:631–639. <https://doi.org/10.1002/bit.10517>.
45. Bae SW, Hong HJ, Lee GM. 1995. Stability of transfectomas producing chimeric antibody against the pre-S2 surface antigen of hepatitis B virus during a long-term culture. *Biotechnol Bioeng* 47:243–251. <https://doi.org/10.1002/bit.260470216>.
46. Chuck AS, Palsson BO. 1992. Population balance between producing and nonproducing hybridoma clones is very sensitive to serum level, state of inoculum, and medium composition. *Biotechnol Bioeng* 39:354–360. <https://doi.org/10.1002/bit.260390315>.
47. Frame KK, Hu WS. 1990. The loss of antibody productivity in continuous culture of hybridoma cells. *Biotechnol Bioeng* 35:469–476. <https://doi.org/10.1002/bit.260350504>.
48. Lee GM, Varma A, Palsson BO. 1991. Application of population balance model to the loss of hybridoma antibody productivity. *Biotechnol Prog* 7:72–75. <https://doi.org/10.1021/bp00007a013>.
49. Hammill L, Welles J, Carson GR. 2000. The gel microdrop secretion assay: identification of a low productivity subpopulation arising during the production of human antibody in CHO cells. *Cytotechnology* 34:27–37. <https://doi.org/10.1023/A:1008186113245>.
50. Pallavicini MG, DeTeresa PS, Rosette C, Gray JW, Wurm FM. 1990. Effects of methotrexate on transfected DNA stability in mammalian cells. *Mol Cell Biol* 10:401–404. <https://doi.org/10.1128/mcb.10.1.401-404.1990>.
51. Kim SJ, Kim NS, Ryu CJ, Hong HJ, Lee GM. 1998. Characterization of chimeric antibody producing CHO cells in the course of dihydrofolate reductase-mediated gene amplification and their stability in the absence of selective pressure. *Biotechnol Bioeng* 58:73–84. [https://doi.org/10.1002/\(SICI\)1097-0290\(19980405\)58:1%3C73::AID-BIT8%3E3.0.CO;2-R](https://doi.org/10.1002/(SICI)1097-0290(19980405)58:1%3C73::AID-BIT8%3E3.0.CO;2-R).
52. Dobzhansky T. 1936. Position effects on genes. *Biological Rev* 11:364–384. <https://doi.org/10.1111/j.1469-185X.1936.tb00911.x>.
53. Lewis EB. 1950. The phenomenon of position effect. *Adv Genet* 3:73–115. [https://doi.org/10.1016/s0065-2660\(08\)60083-8](https://doi.org/10.1016/s0065-2660(08)60083-8).
54. Hsieh S-C, Liu I-J, King C-C, Chang G-J, Wang W-K. 2008. A strong endoplasmic reticulum retention signal in the stem-anchor region of envelope glycoprotein of dengue virus type 2 affects the production of virus-like particles. *Virology* 374:338–350. <https://doi.org/10.1016/j.virol.2007.12.041>.
55. Chiou S-S, Crill WD, Chen L-K, Chang G-JJ. 2008. Enzyme-linked immunosorbent assays using novel Japanese encephalitis virus antigen improve the accuracy of clinical diagnosis of flavivirus infections. *Clin Vaccine Immunol* 15:825–835. <https://doi.org/10.1128/CVI.00004-08>.
56. Tsai W-Y, Driesse K, Tsai J-J, Hsieh S-C, Sznajder Granat R, Jenkins O, Chang G-J, Wang W-K. 2020. Enzyme-linked immunosorbent assays using virus-like particles containing mutations of conserved residues on envelope protein can distinguish three flavivirus infections. *Emerg Microbes Infect* 9:1722–1732. <https://doi.org/10.1080/22221751.2020.1797540>.
57. Matasci M, Hacker DL, Baldi L, Wurm FM. 2008. Recombinant therapeutic protein production in cultivated mammalian cells: current status and future prospects. *Drug Discov Today Technol* 5:e37–e42. <https://doi.org/10.1016/j.ddtec.2008.12.003>.
58. Roehrig JT, Bolin RA, Kelly RG. 1998. Monoclonal antibody mapping of the envelope glycoprotein of the dengue 2 virus, Jamaica. *Virology* 246:317–328. <https://doi.org/10.1006/viro.1998.9200>.
59. Calvert AE, Bennett SL, Dixon KL, Blair CD, Roehrig JT. 2019. A monoclonal antibody specific for Japanese encephalitis virus with high neutralizing capability for inclusion as a positive control in diagnostic neutralization tests. *Am J Trop Med Hyg* 101:233–236. <https://doi.org/10.4269/ajtmh.19-0073>.
60. Hall RA, Burgess GW, Kay BH, Clancy P. 1991. Monoclonal antibodies to Kunjin and Kokobera viruses. *Immunol Cell Biol* 69:47–49. <https://doi.org/10.1038/icb.1991.7>.
61. Henchal EA, Gentry MK, McCown JM, Brandt WE. 1982. Dengue virus-specific and flavivirus group determinants identified with monoclonal antibodies by indirect immunofluorescence. *Am J Trop Med Hyg* 31:830–836. <https://doi.org/10.4269/ajtmh.1982.31.830>.
62. Heckman N, Lockhart R, Nielsen JD. 2013. Penalized regression, mixed effects models and appropriate modelling. *Electron J Statist* 7:1517–1552. <https://doi.org/10.1214/13-EJS809>.
63. Ruppert D, Wand MP, Carroll RJ. 2003. *Semiparametric regression*. Cambridge University Press, New York, NY.
64. Bassett G, Koenker R. 1982. Tests of linear hypotheses and L1 estimation. *Econometrica* 50:1577–1583. <https://doi.org/10.2307/1913398>.
65. R Development Core Team. 2021. R: a language and environment for statistical computing, v4.1.0. R Foundation for Statistical Computing, Vienna, Austria.
66. Chiou S-S, Fan Y-C, Crill WD, Chang R-Y, Chang G-JJ. 2012. Mutation analysis of the cross-reactive epitopes of Japanese encephalitis virus envelope glycoprotein. *J Gen Virol* 93:1185–1192. <https://doi.org/10.1099/vir.0.040238-0>.